Electric Power Systems Research 244 (2025) 111547

Contents lists available at ScienceDirect

Electric Power Systems Research

journal homepage: www.elsevier.com/locate/epsr

Algorithm for distribution network reconfiguration and reactive power compensation with battery energy storage systems

Tomislav Rajić *, Branko Stojanović

University of Belgrade-School of Electrical Engineering, Bulevar kralja Aleksandra 73, Belgrade 11000, Serbia

ARTICLE INFO

Keywords:
Reconfiguration
Kruskal algorithm
Simulation annealing
Battery energy storage systems

ABSTRACT

The paper deals with distribution network reconfiguration and reactive power compensation, taking into account the existence of distributed energy sources, Distributed Generation and Battery Energy Storage Systems. A large number of constraints are included in order to present the problem as realistically as possible. The limitations are the satisfaction of the input power factor, non-overcompensation with reactive power, the minimum and maximum value of the voltage in the nodes, the maximum allowed effective value of the network branch currents and the number of commutations per switching element within 24 h. Contributions are realistic representation of hourly changes in consumption and production from renewable energy sources and BESS, alongside reconfiguration (with commutaton constraint), what is rarity in modern works. The idea of the paper is to present the method that combines the Kruskal algorithm for reconfiguration and the Simulated Annealing (SA) for compensation. The optimization method determines the position of the capacitor banks and the network configuration that minimizes active power losses and cost on an hourly basis. Detailed analyses show how BESS affect technically optimal solution and what is the final cost. The addressed problem is of Mixed Intiger Nonlinear Programming optimization class.

1. Introduction

The problem of distribution network reconfiguration has become particularly relevant since the advent of renewable energy sources, Distributed Generation. Consequently, distribution networks will not have one direction power flow. Losses in distribution networks are significant, making their reduction of vital importance. Overcoming of supply uncertainty, along with variable load demand, make challenge for engineers who manage the power grid. Review papers on the topic of network reconfiguration are [1,2]. In literature many algorithms are mentioned for solving network reconfiguration problem. They can be broadly classified as: 1) heuristic methods [3–5] or a combination of heuristics (experimental, non-mathematical knowledge) and other optimization methods [6–8], 2) metaheuristic methods [9,10], 3) artificial intelligence-based methods [11,12], and 4) mathematical methods [13]. The algorithm described in this paper is heuristic. It addresses the minimization of network active power losses and the cost of capacitor batteries. The presented solution belongs to dynamic reconfiguration methods when it is done each hour [2]. The analyzed problem is of Mixed Intiger Nonlinear Programming (MINLP) optimization class. Special contribution is the inclusion of DG and Battery Energy Storage Systems.

The most recent references deal with concurrent placement of capacitors, network reconfiguration and DG allocation [14,15]. Very fast static simultaneous capacitor placement and network reconfiguration algorithm surpassing nonlinear metaheuristic time consuming approaches is presented [14]. This is achieved by transforming polynomial load formulations into quadratic ones. Voltage dependent load model for industrial, residential, commercial and mixture patterns for low size (16 and 33 bus) networks was employed. The proposed model was introduced through CPLEX within AMPL software solver and is much less time consuming than KNITRO. In [15] within the framework of AMPL (A Mathematical Programming Language), employing a daily load profile for both active and reactive demand, using linear solvers, concurrent optimization of capacitor placement, network reconfiguration with biomass distributed generation is performed. Economic issue is included in the analysis. All nonlinear variables have been substituted by their squared values. Low size distribution networks were considered, up to 30 nodes.

Few authors deal with the reconfiguration of the distribution

* Corresponding author.
E-mail address: rajic@etf.rs (T. Rajić).

https://doi.org/10.1016/j.epsr.2025.111547
Received 18 August 2024; Received in revised form 19 January 2025; Accepted 14 February 2025
Available online 20 February 2025

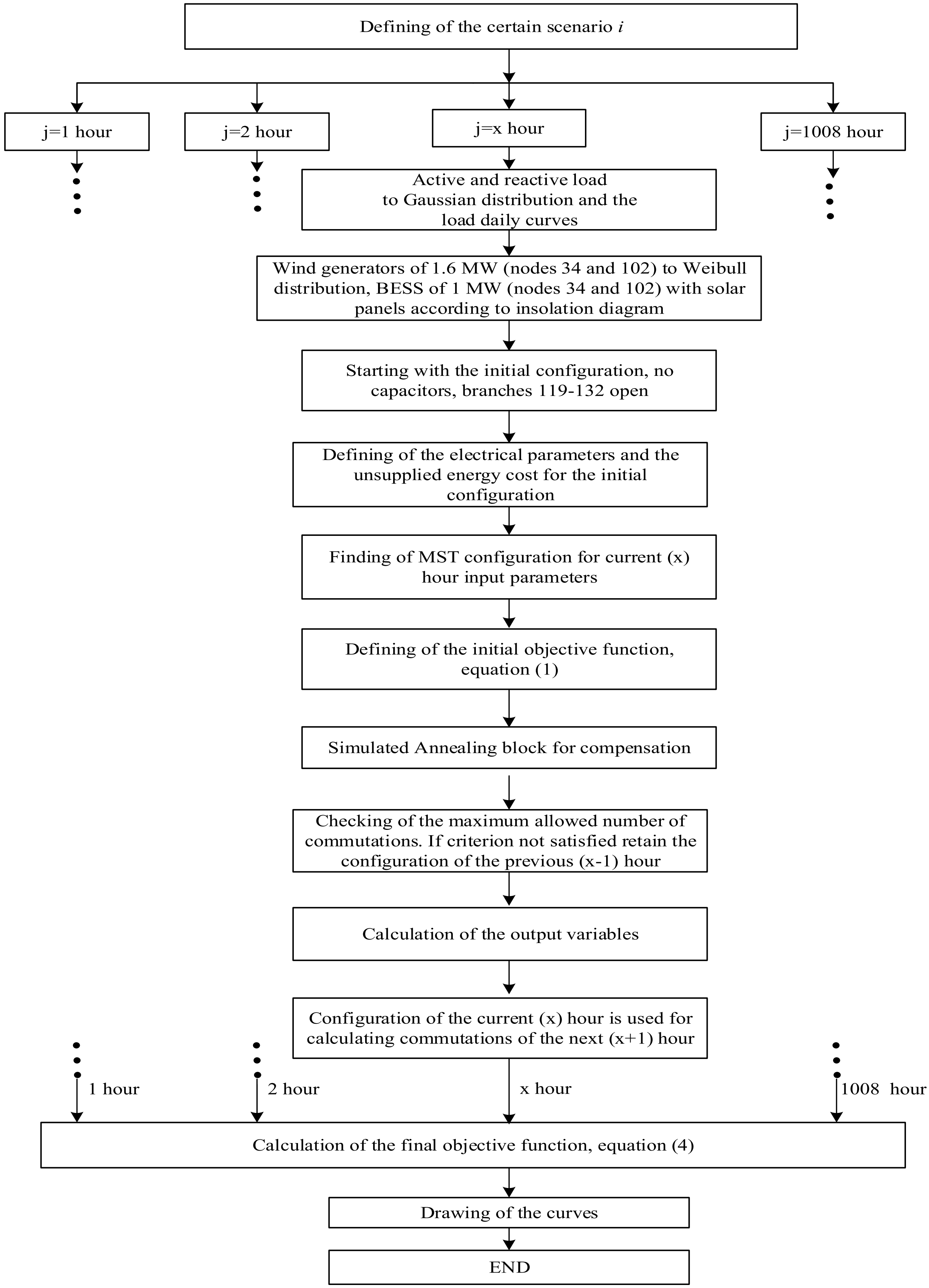

Fig. 1. MST plus SA, hybrid algorithm.

network on an hourly basis [16]. Solar irradiance is treated stochastically for each hour using Markov model [17]. The resilience of active distribution network with reconfiguration is the subject of [18], while the virtualization of micro-PMU devices for changing network topology is presented in [19]. Like previous works, this paper follows current trends. The stochastic nature of power generation from DG must be considered when planning the configuration of the distribution network for each hour. In addition to DG, the perspective of distribution networks also includes BESS. There are several papers addressing the presence of BESS [20] (Hydrogen Energy Systems-HES) and [21]. Weakly meshed distribution network with voltage variation in the range 0.81–1.21 p.u. is presented in [20]. In [21] idle run of BESS is also considered. The economic aspect of this problem is rarely considered [20,22]. Eleven load models are exposed in [22] for period of DG lifespan.

Authors usually tend to choose the different network constraints. It is necessary to consider a great number of them to represent the problem as realistically as possible. In addition to mandatory current and voltage constraints, others must also be analyzed. One rarely used constraint is the number of switch operations per day [23]. The drawback of the paper [23] is that a limited number of commutating branches of large scale distribution network is analyzed. The constraint of commutations is crucial because too many operations can lead to equipment wear and reduced lifespan.

For testing employed algorithms authors usually use IEEE test networks of 33 or 69 nodes [24,25]. The pioneering work in [24] is that binary reconfiguration variables are presented as continuous ones in the unbalanced grid. Minimizing the power loss and maximizing voltage stability index by linearization of non linear distribution network equations for power flow, voltages and currents is performed in [25]. Some authors make contribution considering demand variability [26, 27]. Reconfiguration with simultaneous planning of DG is given by voltage dependent model in [26]. An impressive method for the losses decrease and to alleviate undesirable consequences of DG wrong placement is reconfiguration when topology is altered with predicted DG power and load which are subject to technical and operational restrictions and it is submitted in [27]. Standard deviation in generation of the solutions which are better than in previous literature in proposed model [27], is zero.

Objective of the paper is forming an algorithm for reconfiguration of distribution power network and reactive power compensation, taking into account the presence of distributed energy sources and storage systems. A large number of constraints are included in order to present the problem as realistically as possible. The limitations are the satisfaction of the input power factor, non-overcompensation with reactive power, the minimum and maximum value of the voltage in the nodes, the maximum allowed effective value of the network branch currents and the number of commutations per switching element within 24 h. Renewable energy sources connected via inverters and BESS could produce absolutely some reactive power. But, renewable sources can generate some energy (active and reactive) only during windy or sunny hours. Capacitor banks are independent reactive power sources. Further, BESS are far more expensive than capacitor banks. This paper assumes that all of the DG and BESS units are operating with power factor equal to one. Albeit there is possibility for injecting reactive power in the grid via inverters, capacitor banks can assure more tight regulation of network input power factor and voltage profile.

This paper employ combination of two algorithms to form the new one and optimization is performed at two levels. First, Kruskal algorithm is applied to solve the network reconfiguration problem, followed by Simulated Annealing [28] for the compensation problem of the reactive power. Existing network reconfiguration methods typically discard infeasible solutions until a feasible one is generated, which captures the most computational time. Therefore, the paper adopts Kruskal algorithm to build a Minimum Spanning Tree (MST) [29].

In the presented paper the measurements from a real substation in Belgrade, Serbia are used. This observation is important to follow consumption variations per day during the monitoring. Based on these assumptions characteristic working and non-working day consumptions are given in relative value. This is another contribution of the paper. The power flow calculations were performed using the MATPOWER software within the MATLAB environment.

Main contributions of the paper are such as:

- Algorithm for distribution network reconfiguration in order to minimize power losses and total costs.
- Using capacitor banks for reactive power compensation and determination of their positions.
- Consideration of stochastic nature of production and consumption of large scale distribution network (118 bus test system) each hour, for long time period (1008 h).
- Reconfiguration analysis is done per hour basis.
- Proper analyses of BESS (with unique charging/discharging presentation) which reflect the future of distribution networks.
- Considering the maximum allowed number of commutations per switching element for 24 hour period in reconfiguration analysis.

The organization of the paper is as follows: Section 2 gives algorithm description. Section 3 introduces test network. Section 4 covers comparison of two different algorithms employed herewith. Modeling of consumption and generation from renewable energy sources is presented in Section 5 followed by insight in BESS location determination in Section 6. Results are depicted in Section 7. Review of recent works on similar topic is elaborated in Section 8. The paper is concluded with Section 9.

2. Algorithm description

The authors employ combination of two algorithms to form the new one and optimization is performed at two levels. First, Kruskal algorithm is applied to solve the network reconfiguration problem, followed by Simulated Annealing for the compensation problem of the reactive power. Existing network reconfiguration methods typically discard infeasible solutions until a feasible one is generated, which captures the most computational time. Therefore, the paper adopts Kruskal algorithm to build a Minimum Spanning Tree (MST) [29]. It is applied each hour and the achieved configuration is radial.

Algorithm can be briefly described as follows:

- For a fully meshed network, effective branch currents are determined, which become weight coefficients.
- The branch with the highest weight coefficient is closed, provided that no loop is formed.
- The newly created node is recorded in the set of nodes.
- If all network nodes have been visited, the algorithm stops.
- If not, the process continues with the same logic until all network nodes are visited.

Simulated Annealing is slower than another optimizing algorithms, but fast enough and easy for incorporation of so many constraints such as simultaneous incorporation of the DGs, BESS, capacitor banks, numbers of commutations etc. Furthermore Simulated Annealing algorithm is efficient for solving large-scale problems, when there is not radiality constraint.

Notable observation can be made that there is only one power flow calculation, what is the reason why the algorithm is exceptionally fast. For the IEEE network with 118 nodes, the computation time is of 1 second order. Fig. 1 shows the diagram for the applied algorithm, step by step from start to the end. The final step is the program exit. All active power losses in the algorithms are calculated using an efficient power flow method of the MATPOWER environment.

The five crucial chronological steps should be underscored:

Table 1
Comparative analysis for obtaining optimal solution by different algorithms from the literature.

Algorithm	Ploss [kW]	Open branches	Calculation time
Result in literature	869.8	42, 26, 23, 51, 122, 58, 39, 95, 74, 71, 97, 129, 130, 109 i 34	1283.4 s
SA	917.6	129, 109, 95, 87, 85, 76, 72, 61, 52, 47, 42, 38, 33, 25 i 21	17 days
MST	894.5	22, 26, 34, 39, 42, 50, 58, 71, 73, 75, 95, 109, 122, 129 i 130	1 s

- Wind generator nodes allocation by Monte Carlo method;
- PV nodes determination by heuristic method;
- BESS nodes placement (detailed discussion is given in Section 6);
- Application of MST algorithm for reconfiguration problem and
- Adoption of SA method for compensation problem.

Objective Functions:

The network is analyzed for 1008 h of operation. It is assumed that the number of operating hours is divisible by 24 to account for whole days (1008 h = 42 days). There are two parts of objective function. One part is the minimization of losses, and the other is the minimization of costs.

The objective function at each hour is:

$$\min FINALCOST_{i,j}[\$] = 0.15 \cdot E1_{i,j} + 120 \cdot P_{loss,i,j} + C_{\text{int},i,j} \tag{1}$$

Where:

$E1_{i,j}$[$] - the price of capacitor batteries,

0.15 - the annual capacitor inerest rate,

120 [$/kW] - the penalty for active power losses,

$P_{loss,i,j}$[kW] - active power losses,

$C_{int,i,j}$ [$] - cost of unsupplied electric energy,

j - index relating to the current hour and

i - index relating to the current scenario.

In the objective function, for each hour of operation, the cost for commutations during the hour of operation is neglected because of its negligibility to the other summations in equation as well as the cost of BESS charge/discharge (1).

$$C_{\text{int},i,j} = c_{\text{int}} \cdot \alpha \cdot d \cdot \sum_{q \in N_b} \lambda_q \cdot l_q \cdot \text{Re}\{I_{q,i,j}\} \cdot \sqrt{3} \cdot U_r, \forall i \in I, j \in J. \tag{2}$$

In expression (2), the following notations are used: cint - penalty for the unsuppplied electric energy (4$/kWh),

α - load factor (0.6), d - duration of repair (1h),

λ_q - the failure rate of the corresponding network branch (0.0001 faults/km),

l_q - length of branch q (km), for simplicity, 100 km was adopted for the length of each network branch,

Nb - number of network branches,

Iq,i,j - the effective value of the current of branch q in the ith scenario and the jth hour (A),

Ur - nominal network voltage (11 kV),

I - set of all scenarios,

J - set of all network hours.

The cost of unsupplied electric energy, Eq. (2), is derived under the assumption that in the case of a radial distribution network, the interruption of one branch results in the interruption of the supply of all consumers, who are below that branch, that is, "downstream" of the interrupted branch.

Hourly savings are calculated as:

$$SAVINGS_{i,j} = INITIAL_{i,j} - FINALCOST_{i,j} \tag{3}$$

where $INITIAL_{i,j}$ is the initial objective function for the starting configuration (without commutations and without capacitor banks).

The objective function for the entire observed period of 1008 h is given by the expression:

$$\begin{aligned} ENERGYSAVINGS_i[\$] = {} & 120 \cdot \max\left(P_{loss,initial,i,j}\right) + 0.03 \cdot \sum_{j=1}^{N^{hours}} P_{loss,initial,i,j} + \sum_{j=1}^{N^{hours}} C_{\text{int},initial,i,j} - \\ & + \left[0.15 \cdot E1_{i,j} + 120 \cdot \max\left(P_{loss,i,j}\right) + 0.03 \cdot \sum_{j=1}^{N^{hours}} P_{loss,i,j} + \sum_{j=1}^{N^{hours}} C_{\text{int},i,j} + C_{com,i} + BESS\right] \end{aligned} \tag{4}$$

In (4) is assumed:

0.03 [$/kWh] - the cost of losses of the supplied electric energy,

Ccom,i - the price of commutations (the price of one commutation is $1 or $50). Calculations were made for the both and

BESS - BESS cost of charge and discharge for 1008 hour period.

In the exploitation and planning of distribution networks, the scenario that has the least cost is sought, within all technical conditions.

Constraints

- The voltage in each node must be in the range of 0.95–1.1 p.u.
- The currents must not be higher than those provided for each branch.
- Maximum and minimum power of built-in capacitor batteries.
- The input power factor of the entire network must not be <0.85.
- The number of commutations per switching element within 24 h must not exceed 6.

3. Test network

For the purpose of testing the algorithm, the IEEE test network of 118 nodes and 132 branches was used. This network is known in the literature [32]. Total losses after calculation of power flow for initial configuration amount to Ploss=1298.1 kW. The computation was performed on the original network without added renewable energy sources, capacitors and BESS. The initial configuration means that branches 118–132 are open. The basic power is 100 MVA and the nominal voltage is 11 kV. The lowest voltage is in node 76 and is 0.869 p.u. The new algorithm will improve voltage conditions and reduce currents through network branches. Complete description of the tested network with pertaining data are given in the **Appendix**.

The "curse of immensity" can be encountered when dealing with large scale distribution networks compared to low (33 bus) and medium (69 bus) grids regarding computational burden and population size which is of $\binom{n}{k}$ order where n stands for the total number of commutating branches and k for corresponding ties. The total number of branches is one less than the number of buses in radial networks with one slack node. The smaller number of buses leads to "curse of immensity" being less exposed. It is overcome in the case of 118 bus tested network, by Kruskal scalable algorithm usage. A bigger network is closer to the realistic distribution network.

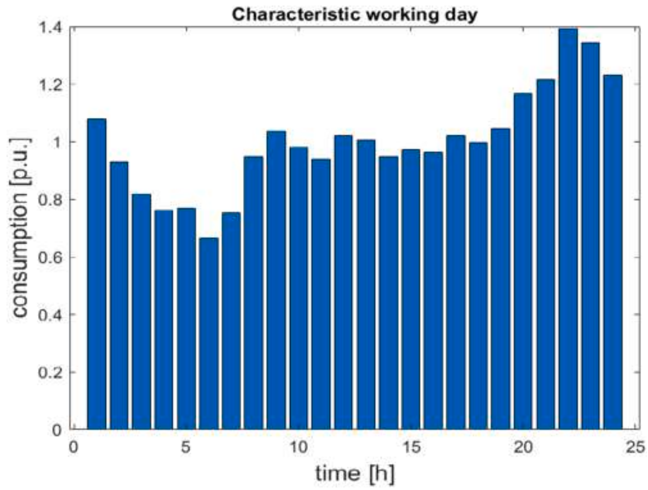

Fig. 2. Typical consumption curve for a working day.

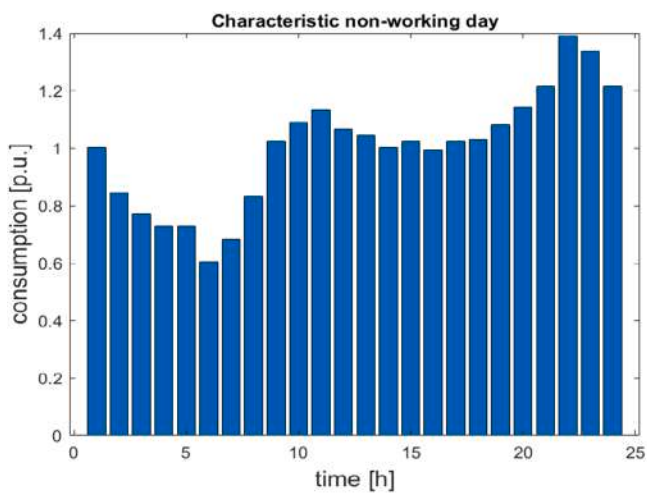

Fig. 3. Typical non-working day consumption curve.

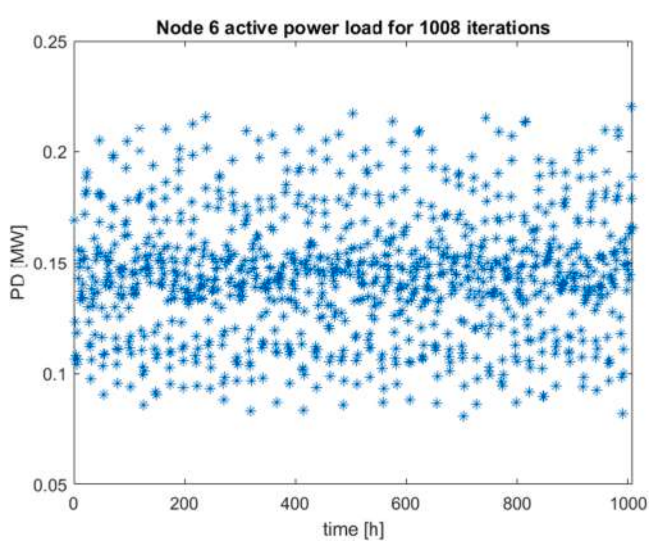

Fig. 4. Node 6 active power load vs. time.

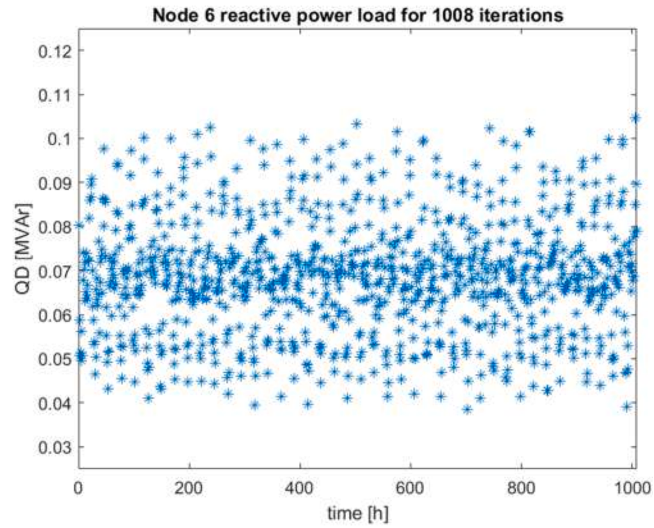

Fig. 5. Node 6 reactive power load vs. time.

4. Comparison of two different algorithms

On the 118-node test network, two different approaches were applied to perform a direct comparison of the two algorithms concerning reconfiguration for active power loss reduction. Only methods for obtaining the optimal configuration were compared. One approach used Simulated Annealing, and the other used Minimum Spanning Tree. The calculations were performed without including renewable energy sources, capacitors and BESS. The computations were executed on a Pentium IV PC; Intel Core i7–4770, 3.4 GHz; 32 GB RAM. The results are shown in Table 1. Using SA for reconfiguration is completely inadequate for this problem as it lasts too long (17 days) and yields worse result.

This confirmed the fact that MST algorithm provides an approximation of the global optimum in incomparably shorter time, which is not much worse than global optimum. Because of the above, only the algorithm that uses the combination of MST and SA is used, so it is the main topic of this paper. The SA algorithm is used for compensation and the MST for reconfiguration separately.

5. Modeling consumption and production from renewable energy sources

5.1. Modeling consumption

It has been adopted that consumption changes on an hourly basis. Daily consumption curves were used in the network calculations, for both working and non-working day, for an arbitrary urban consumer. Real measurements of consumption changes for a predominantly residential area in the city of Belgrade, Serbia, were used. Consumption is given in relative units of the transformer's nominal power. The measurements were divided into hours, resulting in 24 values for a characteristic working and non-working day. Figs. 2 and 3 show these characteristic days.

To ensure that not all daily profiles are identical, it has been introduced that they vary by 5–10 % from the characteristic day. This was done by using Gaussian distribution in order to simulate consumption from day to day, not to be identical for all. This results in variable consumption that does not deviate much from the characteristic value. The example is closer to real-world scenario. The absolute value equivalent to 1 per unit is equal to the nominal consumption at a given node for the tested network and varies from node to node.

Uncertain variables are active and reactive nodal consumptions. At the beginning expected loads in any node are taken from nominal input data. Deviations from nominal value are regarded as "errors" and by

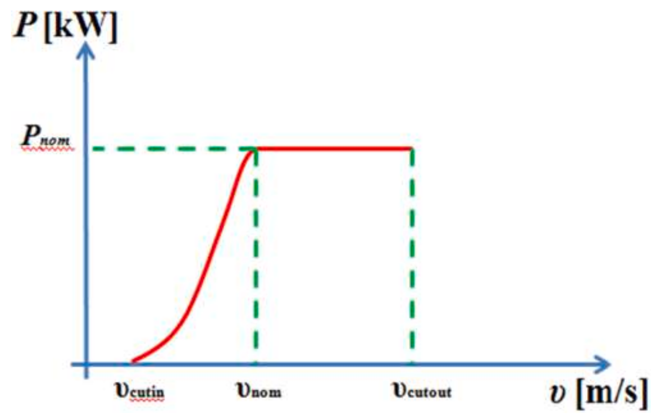

Fig. 6. Produced electrical power of the wind turbine depending on the wind speed.

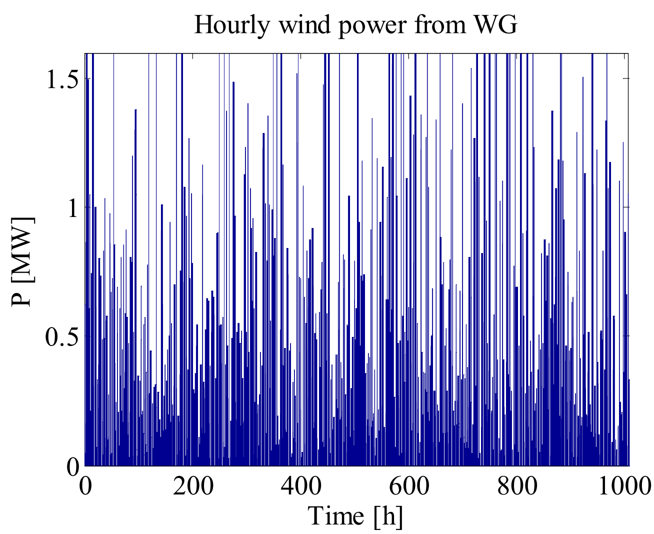

Fig. 7. Hourly wind generator power production for 1008 h.

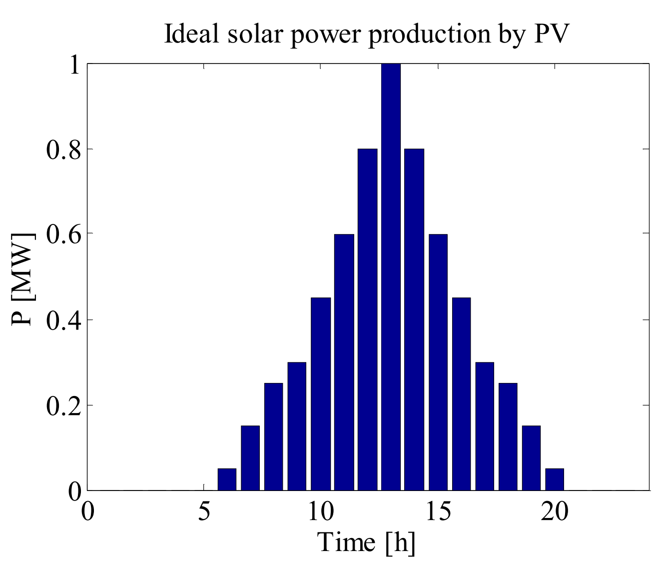

Fig. 8. Ideal daily PV power production.

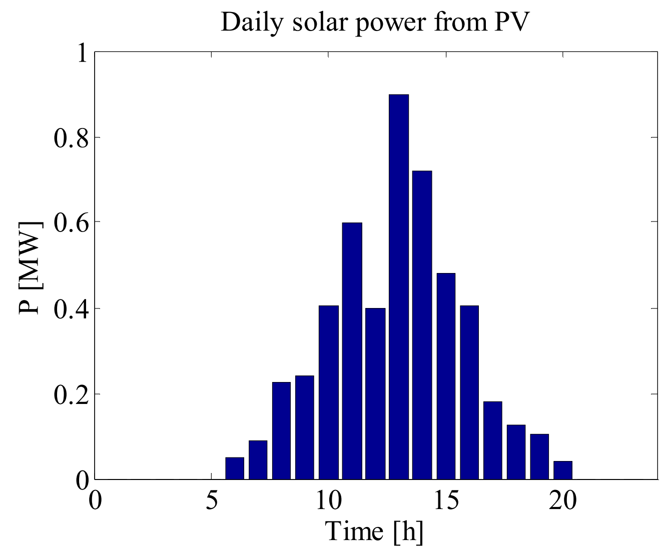

Fig. 9. Realistic daily PV power production.

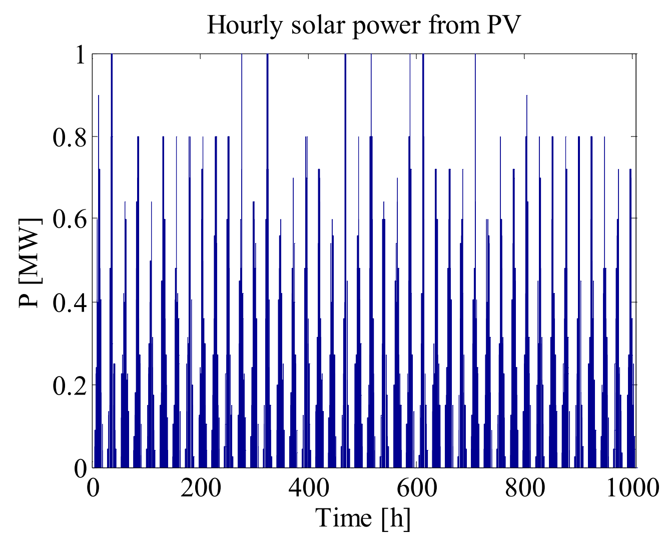

Fig. 10. Hourly PV power production for 1008 h.

"error low" are depicted by Gaussian (Normal) distribution hourly. Standard deviation from expected value is 10 %.

Active and reactive power load for arbitrarily chosen node (node 6) are presented on Figs. 4 and 5 respectively. Important notification regarding the figures is that loads oscillate round their expected (mean, nominal) values 144 kW and 68.6 kVAr conducted by Gaussian distribution.

5.2. Production from wind turbines and photovoltaic panels

When it comes to wind generators, the randomness of their production is defined by the Weibull distribution concerning the probability of wind speed [33]:

$$f(v) = \frac{k}{A}\left(\frac{v}{A}\right)^{k-1} e^{\left(-\left(\frac{v}{A}\right)^{k}\right)} \tag{5}$$

In Eq. (5) are:

v - wind speed [m/s],

A - Weibull scale parameter in m/s, a measure of characteristic wind speed. A is proportional to the mean wind speed and determines the

Table 2
Results of three different analyses of the BESS deployment in the network.

No Case	WG power [MW]	WG location	BESS power [MW]	BESS location	Tehnical caracteristics not satisfied
1	2 × 12	34 and 102	20	72	ΔImax=−343 A; Umax=1.22 p.u.; reverse power flow
2	2 × 11	34 and 102	18	28	ΔImax=−552 A; Umax=1.16 p.u.; reverse power flow
3	2 × 1.6	34 and 102	2 × 1	34 and 102	–

scale of the f(v) curve (A = 6,00 m/s) and

k - Weibull form parameter (k = 2,00).

Fig. 6 shows the production of wind turbines for different wind speeds. For the maximum turbine power value of 1.6 MW was adopted. The maximum turbine power is chosen to be in proportion with the nominal node consumption. This power is presented with next expressions:

$$P = 0 \text{if} \vartheta \leq \vartheta_{cutin}$$

$$P = f(\vartheta) = \frac{1}{2} \cdot \rho \cdot A \cdot \alpha \cdot \vartheta^3 \text{if} \vartheta_{cutin} \leq \vartheta \leq \vartheta_{nom}$$

$$P = P_{nom} \text{if} \vartheta_{nom} \leq \vartheta \leq \vartheta_{cutout}$$

$$P = 0 \text{if} \vartheta_{cutout} \leq \vartheta$$

The wind speed is stochastic value that automatically leads to generated power. Finally, wind turbine power production depends of stochastic wind speed. All productions for 1008 h are presented in Fig. 7.

The production of photovoltaic panels also changes for each hour [36]. The ideal solar irradiation for one day is absolutely symmetrical as shown on Fig. 8. Cloudiness reduces this production. Cloudiness was presented by Gaussian distribution in order to model uncertainty. Because of that, daily PV production for one random day is presented in Fig. 9. This is more realistic situation. For complete interval period of 1008 h, PV production should look like presented in Fig. 10. Maximum PV power is 1 MW. Irradiation during the day is maximum at 1 pm. It deviates from the symmetric curve by 0 to 10 % each hour due to cloudiness. This results in different irradiation values for each hour. During the night, irradiation is zero.

5.3. Place for installation of renewable energy sources

It was assumed that the distributed generators are present from the very start (initially) and the optimization is carried out subsequently. Two wind turbines and two solar panels differing in capacity are selected, chosen according to the node nominal power consumption of the initial network configuration. It was also assumed that the generators are from the same geographical area, so their wind speeds and solar irradiance are the same [30].

The locations of the wind turbines were chosen by Monte Carlo method. The solar panels were placed based on heuristic rule (similar results are obtained by certain mathematical method [31]), selecting the nodes with the highest load. Once the locations and capacities of the distributed units were determined, they remained fixed throughout the subsequent calculation.

Before reconfiguration and compensation, two wind turbines with a maximum power of 1.6 MW each were installed, that is close to 14 % of the active consumption (22.7097 MW), at nodes 34 and 102. There are also two solar panels with maximum power of 1 MW each, installed at the most loaded nodes in the network, nodes 50 and 111.

6. BESS location determination

Energy storage systems are being implemented in distribution networks increasingly. They play an important role in ensuring that electric energy is clean and more efficiently delivered. The use of energy storage batteries is obligation for distribution system operator when there is significant part of renewable energy sources. The method for applying batteries is as follows:

- Define the location of the battery/batteries.
- Define the battery capacity and charging and discharging power for one hour of operation.
- Define the cost of charging and discharging the batteries for one hour of operation.
- Perform power flow calculations and determine the difference between consumption and production without considering the presence of the batteries.
- If the consumption is higher, the battery generates active power, if production is higher, the battery absorbs active power to charge.

With the calculated charging/discharging power of the battery on an hourly basis, the optimization continues. The adopted model is outlined in reference [16] by the following equations:

$$\mathrm{H_aSoC(k+1)} = \mathrm{H_aSoC(k)} + \eta_{ch}\mathrm{P_{ch}(k)\Delta t} - -\mathrm{P_{dis}(k)\Delta t} / \eta_{dis} \quad (6)$$

$$\mathrm{P_{ch-min}} \leq \mathrm{P_{ch}(k)} £ \mathrm{P_{ch-max}} \quad (7)$$

$$\mathrm{P_{dis-min}} \leq \mathrm{P_{dis}(k)} \leq \mathrm{P_{dis-max}} \quad (8)$$

$$\mathrm{P_{ch}(k)P_{dis}(k)} = 0 \quad (9)$$

$$\mathrm{P_{BES}(k)} = \mathrm{P_{dis}(k)} - \mathrm{P_{ch}(k)} \quad (10)$$

The following notification is used:
H_a – BESS energy capacity (kWh),
SoC (k) – BESS state of charge (%),
P_{ch} (k) – charging power (kW),
P_{dis} (k) – discharge power (kW),
η_{ch}, η_{dis} – charging and discharging efficiency (%),
k – iteration number,
Δt – time step,
P_{BES} (k) – the output power of the BESS at time k,
P_{ch_max}, P_{ch_min} – maximum and minimum charging power and
P_{dis_max}, P_{dis_min} - maximum and minimum discharge power.

BESS cannot charge and discharge simultaneously, so at any moment either Pch(k) or Pdis(k) must be 0, Eq. (9). This model was applied. It is worth noting that a sensitivity analysis was conducted to determine the necessary battery power and potential installation locations. Besides batteries, the power of the DG to be connected was also discussed. A brief overview of this research is presented hereafter.

Before reconfiguration and compensation, at the start of the calculations, for 1008 h of network operation, wind generators up to 12 MW maximum power each were assigned to nodes 34 and 102, and solar panels of 1 MW maximum power (each) were assigned to the most loaded network nodes, node 50 and node 111. For the given parameters, the following technical irregularities were observed: the maximum overload of one branch was −343.31 A, the maximum voltage value in one node was 1.2181 p.u., and due to the reversible power flow at the beginning and end of the calculation, the input power factor was negative. This storage system is not technically acceptable because the constraints were not satisfied. In the second example, the power of the wind generators was reduced to 11 MW. The 18 MW BESS was installed in node 28. The 1.05 p.u. load tap changer position was retained. The technical requirements were not satisfied as well. For the BESS position adopted in this study, the nodes where the wind turbines are located were chosen. As active power is always demanded during the daytime, it

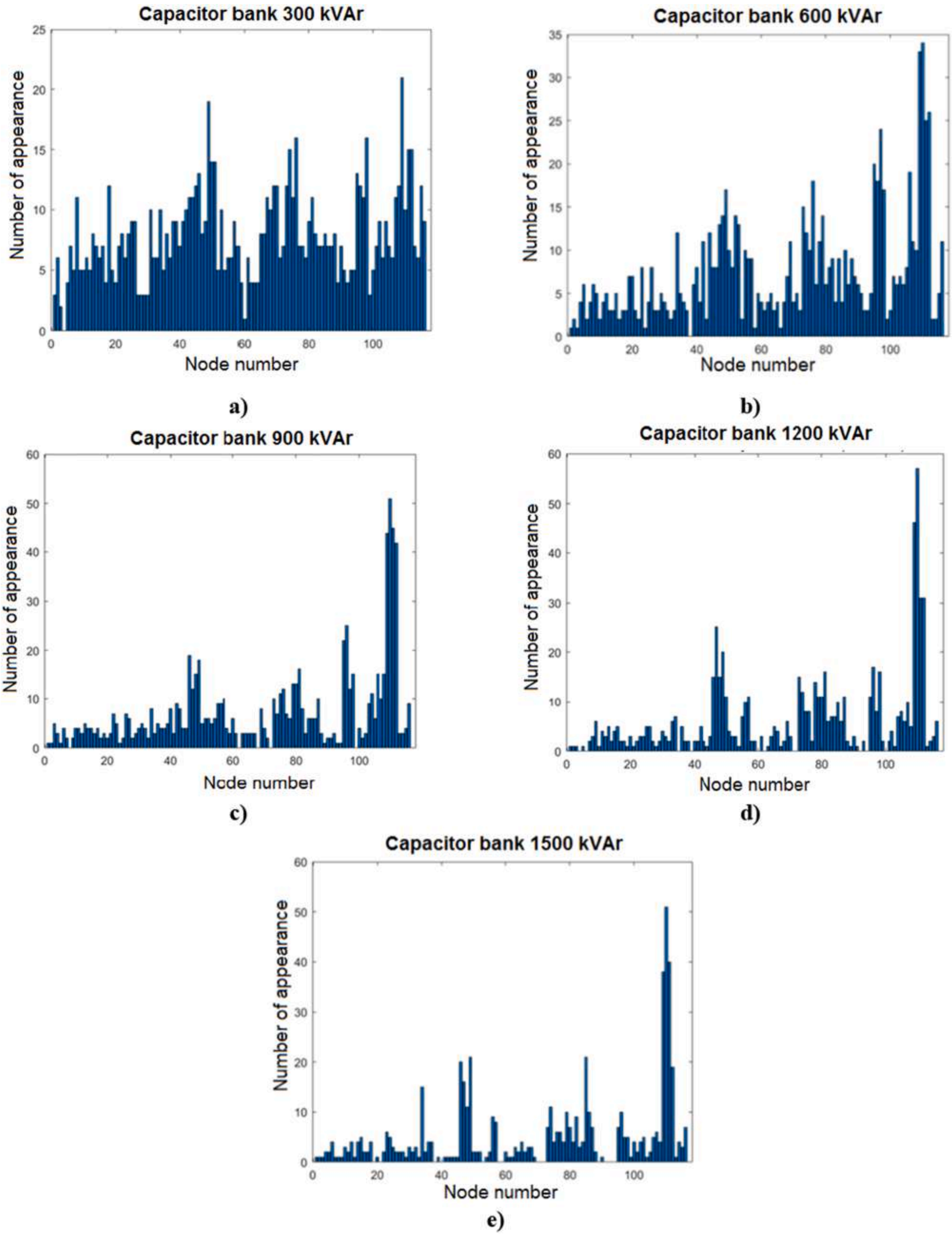

Fig. 11. Switching number for the applied algorithm of: a) 300 kVAr banks b) 600 kVAr banks c) 900 kVAr banks d) 1200 kVAr banks e) 1500 kVAr banks.

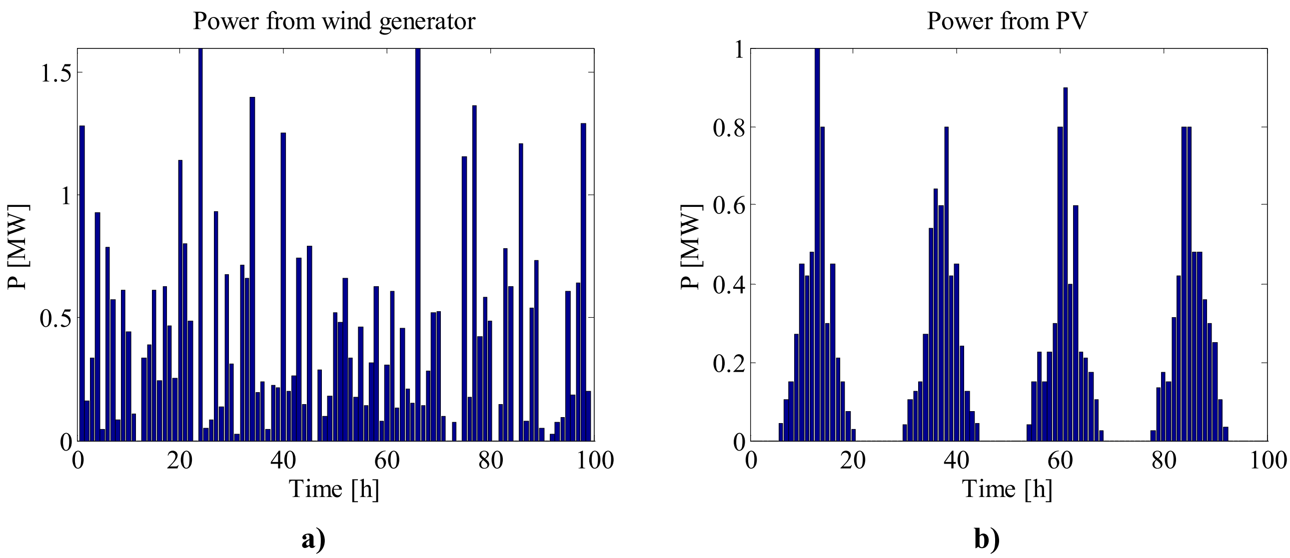

Fig. 12. Hourly power production within 100 h for a) one wind generator and b) one PV panel.

is assumed that the power of the solar panels (PV) will always be utilized during the day hours. The goal is to store wind turbine energy during nighttime hours when consumption is reduced. The BESS are located in the same nodes as the wind generators, charging when their production exceeds node consumption and discharging when their power is too low compared with this consumption. The wind generators are located in nodes 34 and 102, based on Monte Carlo simulation analysis. Their maximum power is 1.6 MW each. The BESS are 1 MW (0.5 MW charging, 0.5 MW discharging) and are located in the same nodes. The solar panels were retained. During the subsequent calculations, only the capacitor banks were varied after the network reconfiguration, which was first performed independently of the compensation. The technical requirements were met. The results of these three previous analyses are presented in Table 2.

From the above, it can be concluded that improper placement of distributed sources and BESS can lead to excessive currents, overvoltages, undervoltages, and power flow reversal. This demonstrates that unplanned placement of BESS can have negative consequences for the system. Therefore, it is very important to pay great attention to planning the battery's position. On the other hand, the research shows that high DG power cannot be connected to the distribution network without determining the optimum to reduce losses and prevent power flow reversal. This problem has been observed in practice and is the subject of many studies [16,17,20,21].

7. Results

During the calculation that followed, only the capacitor banks were varied after the network reconfiguration, which was first performed independently of the compensation. The technical requirements were met. After first phase when capacitors "slide" to the nodes, each hour (Fig. 11) they are assigned to fixed mostly visited nodes, and fixed capacity that is more realistic. Duration of the first phase algorithm on laptop HP 250G9 (Intel Core i5–1235 U up to 4.4 GHz; 8 + 32 GB RAM) is 7 h and 17 mins. Realistic scenarios were built by adding capacitors to network nodes successively, following Fig. 11 it can be observed which nodes are the most visited for each capacitor banks. The new algorithm gives the cheapest solution with minimum power losses. Because of that, only 1200 kVAr, then 600 kVAr and at the end 300 kVAr batteries were assigned to the respective nodes. For clarity sake, time period of 100 h was extracted and Fig. 12 presents hourly power production for one wind generator and one PV panel. The best scenario is shown in Fig. 13.

Figs. 14 and 15 depict the power of the wind turbines and the charging and discharging of the BESS at node 102. Within the algorithm the wind turbine cannot produce >1.6 MW and the BESS cannot charge/discharge at a power greater than half of its maximum capacity in one hour, which is 0.5 MW. These are the maximum values shown in Figs. 14 and 15. Fig. 16 presents power of the BESS at node 102 for 1008 h of network operation.

Inhomogeneous SA parameters are: starting temperature (Tcommencing) 5000 °C, Markov chain length 3000, decreasing temperature rule T = 0.95*T and acceptance ratio 0.001. Hybrid SA-MST algorithm was conducted in MATLAB R2021a environment. The power flow calculations were performed using the MATPOWER software within the MATLAB. Adopted SA algorithm represents no contribution and for this reason is not discussed in detail.

Comparison of different scenarios

A comparison of three scenarios was performed: Scenario 1 (with BESS, Figs. 17 and 18), Scenario 2 (without BESS, Figs. 19 and 20), and the basic, initial Scenario 3 (Figs. 21 and 22) in terms of technical parameters (active power losses and minimum network voltage). High technical quality of generated solutions (Scenarios 1 and 2) in terms of power loss and minimum voltage as well as degradation of basic (initial) Scenario 98 is obvious regarding presented pictures.

The basic scenario is the one that does not contain BESS, capacitor banks (CB) and OLTC. The high technical quality of the generated solution (scenario with BESS) is evident. At the end of this section, the figures showing the switching of branches 50 and 33 for Scenario 1 (Figs. 23 and 24) are presented, indicating that they do not commutate >6 times in 24 h. The calculation results for the mentioned scenarios are presented in Table 3.

The adopted parameters for BESS are [16]:

C_{ch} – 20 $/MWh (charge price),

C_{dis} – 30 $/MWh (discharge price),

BESS charge/discharge cost for 1008 h – 29,672$.

Table 4 shows the adopted cost of capacitor batteries.

The cheapest is Scenario 2, which does not have BESS, and it is cheaper than the identical scenario with BESS for $18,600. It is also significant to note that the scenarios with BESS are costly compared with the ones which do not have it but better in terms of technical characteristics (electrical energy loss, unsupplied electrical energy and peak power losses);

- Components of the objective function Energy (in the middle bracket of the Eq. (4)) for optimal Scenario 2 (without BESS) are:
  1) cost of electrical energy loss $17,328,

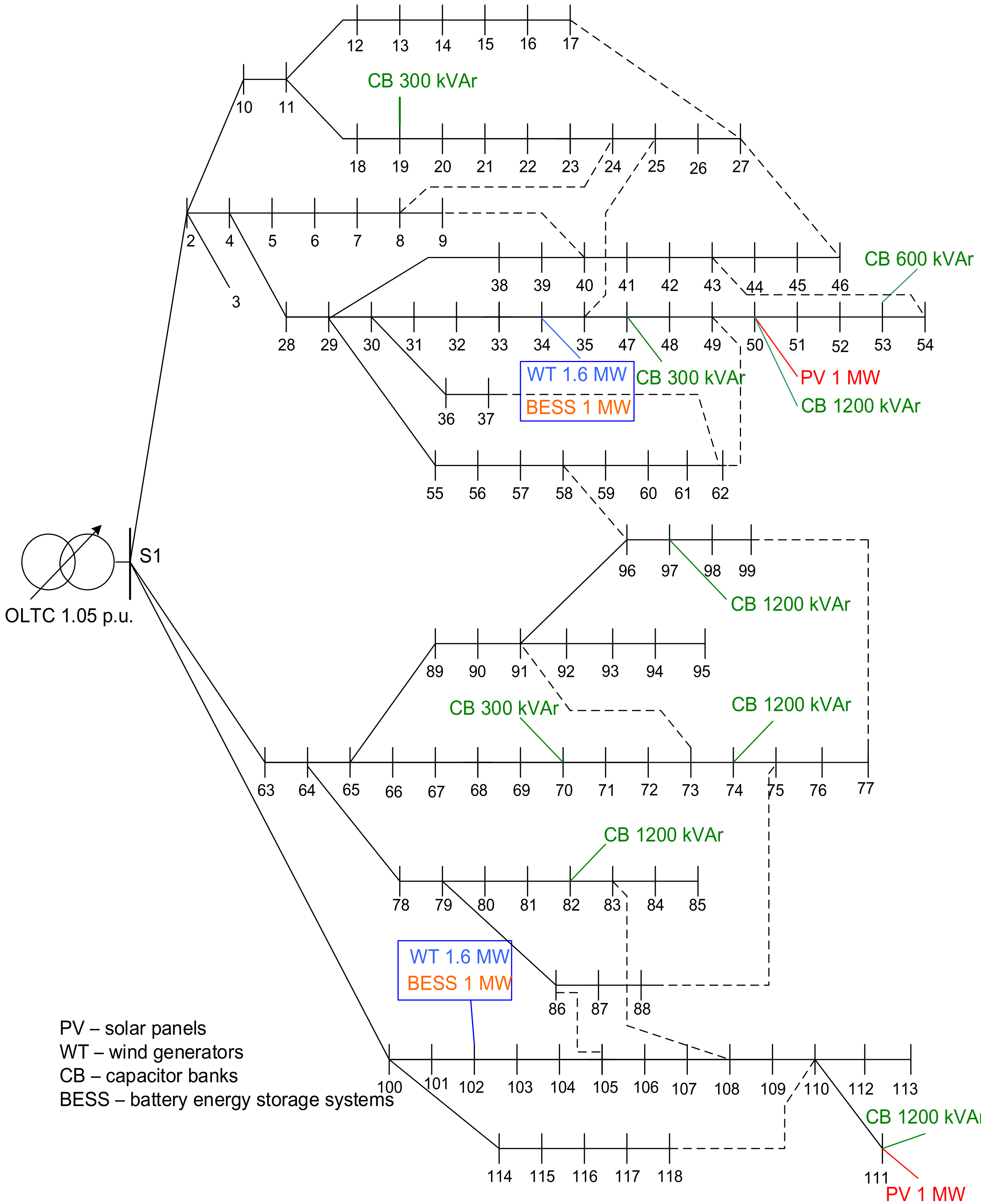

Fig. 13. The best solution with position of all additional elements in the network: DG, BESS, CB and OLTC.

2) cost of unsupplied electrical energy $6486,400,
3) cost of peak power losses $176,960,
4) cost of switching $1459 (cost of commutation $1), and
5) cost of installed capacitor banks $5385.

- Components of the objective function Energy for optimal Scenario 1 (with BESS) are:

1) cost of electrical energy loss $17,316 (better than without BESS by $12),
2) cost of unsupplied electrical energy $6476,000 (better than without BESS by $10,400),
3) cost of peak power losses $176,570 (better than without BESS by $390),

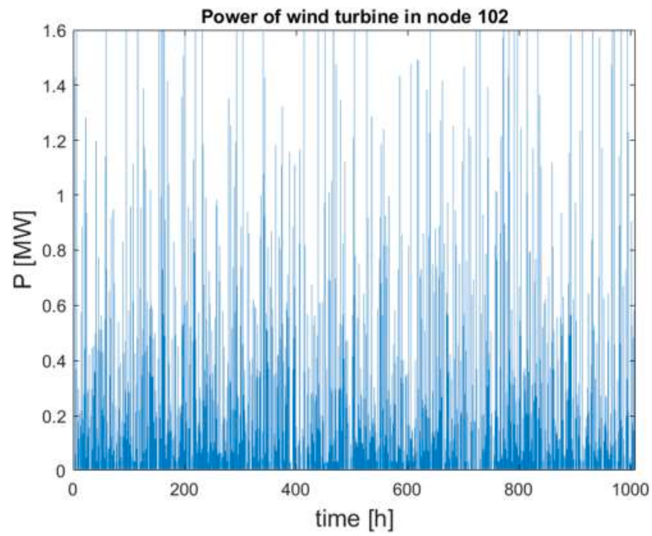

Fig. 14. Production of wind turbine in node 102 for 1008 h of network operation.

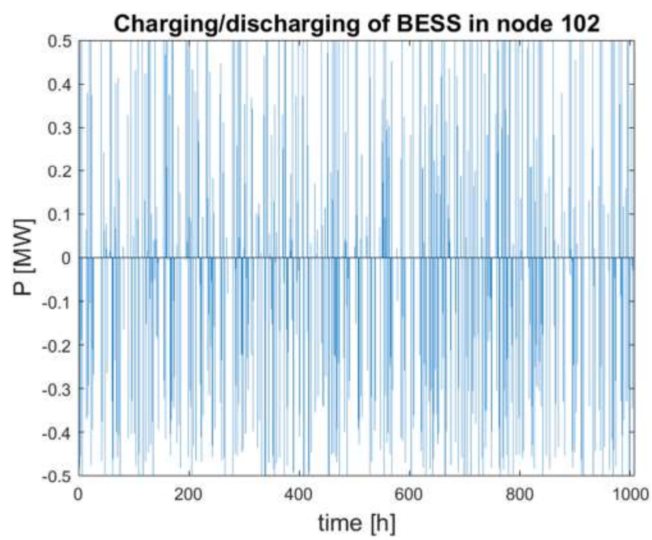

Fig. 15. Charging/discharging of BESS at node 102 for 1008 h of network operation.

4) cost of switching $1189 (cost of commutation $1) (better than without BESS by $270), and
5) cost of installed capacitor banks $5385.

The conclusion is that for the network example, installing BESS with the adopted BESS parameters results in a more expensive Scenario 1 compared to the financially optimal Scenario 2 without BESS. The components of the objective function for Scenario 1 (with BESS) are better (lower in value) than for optimal Scenario 2, indicating that adding Battery Energy Storage Sytems makes full technical sense, especially with regard to the cost of unsupplied electrical energy.

8. Comparison with recent works

By reviewing the literature, a comparison of the proposed approach with other studies has been made. To verify the results, the obtained solutions should be compared with the results of other similar research works. Table 5 shows numerical results of some recent papers with similar topic. Please note that there are no references with identical

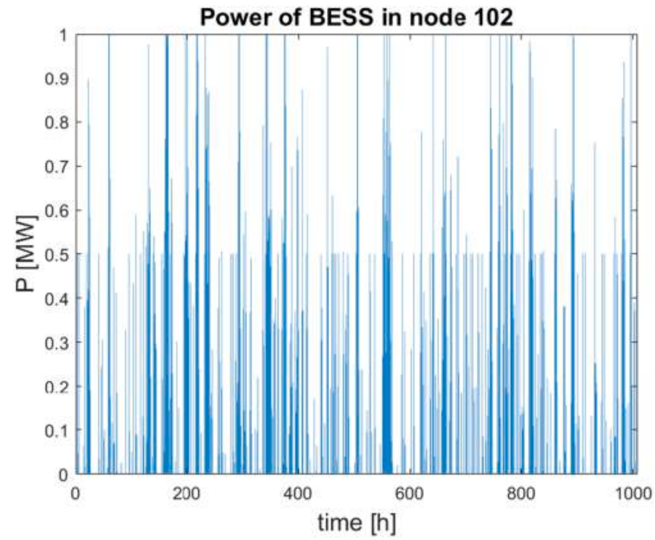

Fig. 16. Power of BESS at node 102 for 1008 h of network operation.

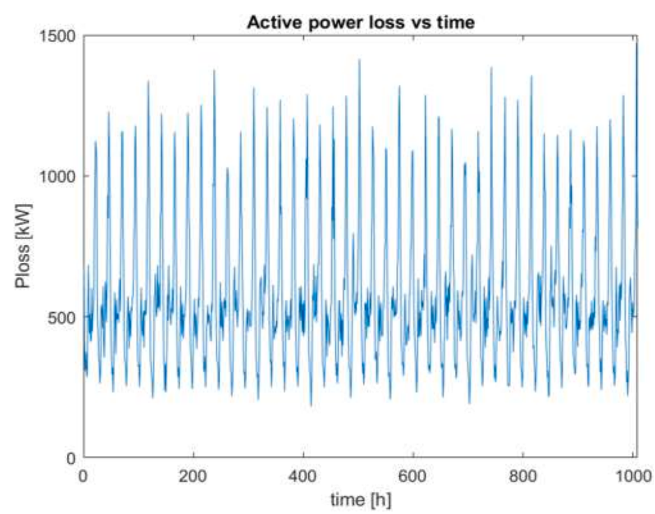

Fig. 17. Active power losses for Scenario 1 within 1008 h (with BESS).

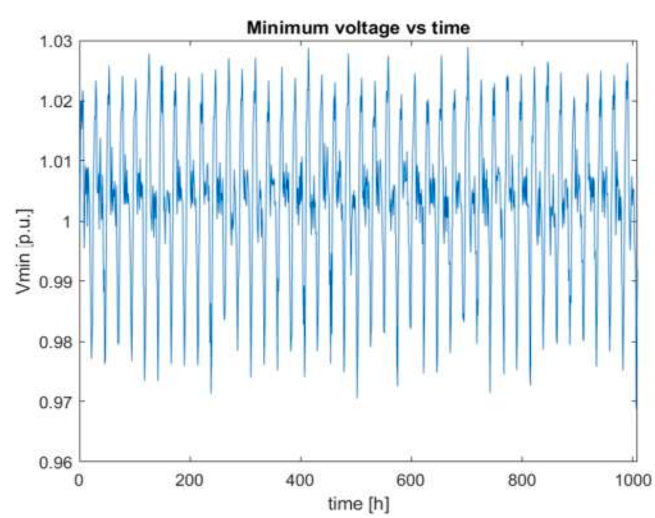

Fig. 18. Minimum voltage for Scenario 1 within 1008 h (with BESS).

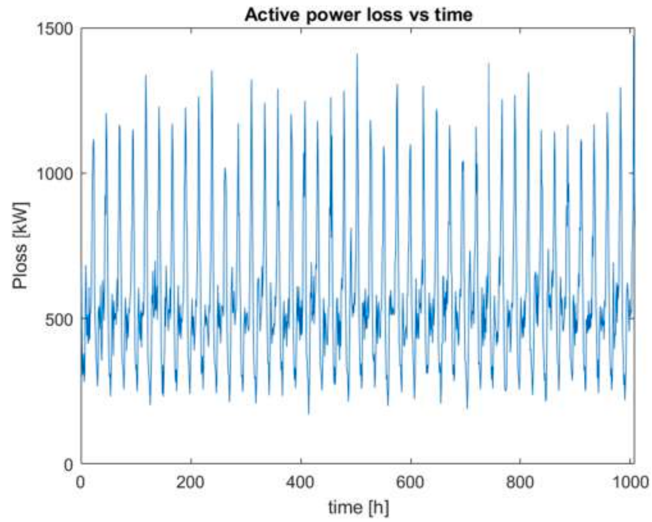

Fig. 19. Active power losses for Scenario 2 within 1008 h (without BESS).

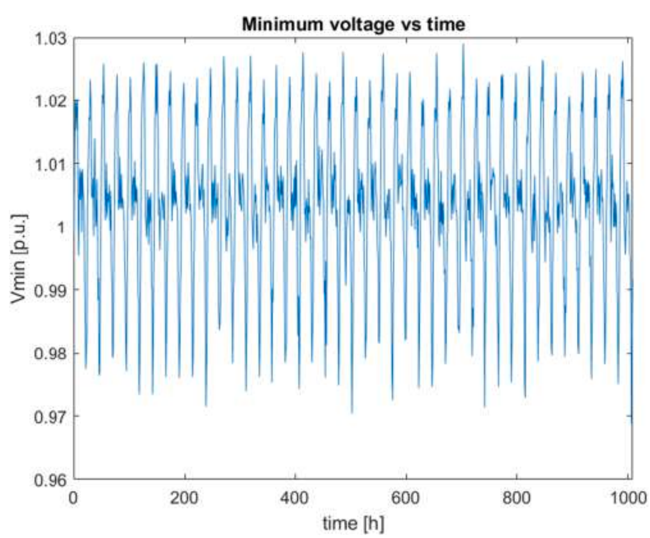

Fig. 20. Minimum voltage for Scenario 2 within 1008 h (without BESS).

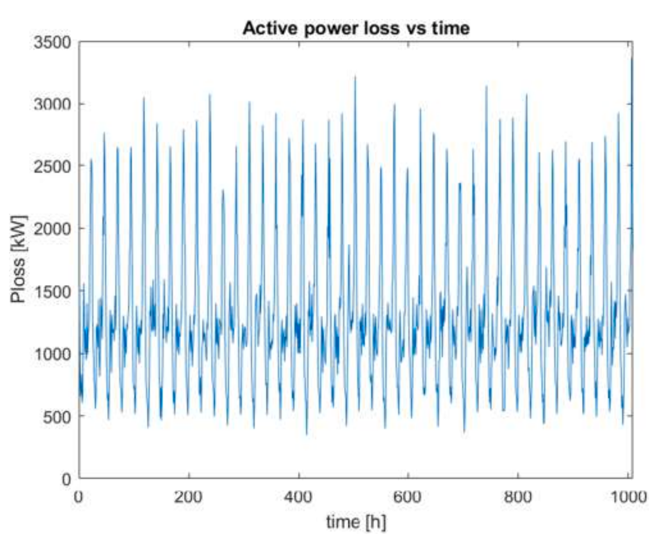

Fig. 21. Loss of active power for Scenario 3 within 1008 h (basic scenario, initial one).

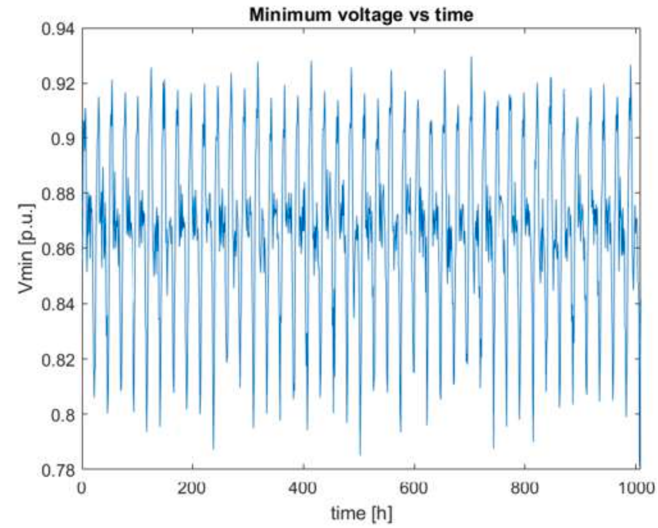

Fig. 22. Minimum voltage for Scenario 3 within 1008 h (basic scenario, initial one).

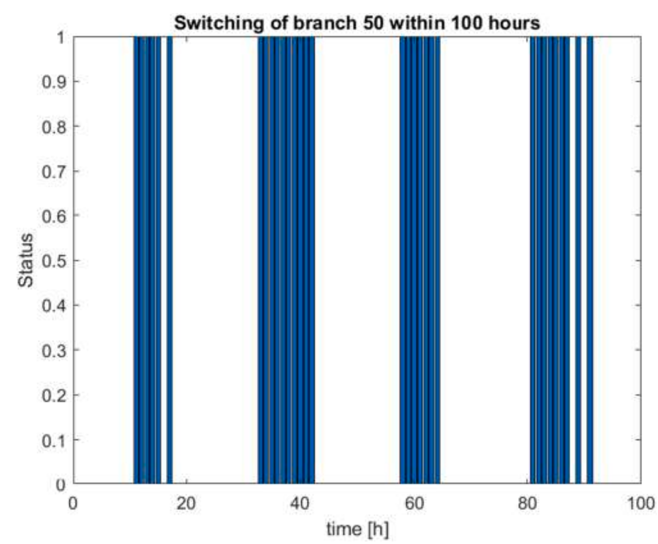

Fig. 23. Hourly closing/opening of branch 50, Scenario 1 for first 100 h.

parameters: whether analyzed network is not the same, DGs are not the same, BESS are not incorporated, constraints are not the same etc. Further, speaking about methodology and considered parameters and power generators, Table 6 gives more detailed information. Table 6 presents a comparison with some solutions to the similar problem, in terms of constraints and analyzed factors. In the first column of Table 6, the reference ordinal number is given. The comparison was made in relation to the following segments: Voltage profile (VP), Economical issues (EI), Load unbalance (LU), Capacitor placement (CP), Load model (LM), DG wind generators presence (DGW), DG solar panels presence (DGS), Number of circuit breaker commutations (CBC), Battery energy storage systems (BESS) or Hydro energy sources (HES). As can be seen, the presented algorithm analyzes the given problem (reconfiguration and compensation) to a significant extent when compared with similar methods in the literature.

9. Conclusion

The paper addresses the topic of reconfiguration of distribution power network and reactive power compensation, taking into account

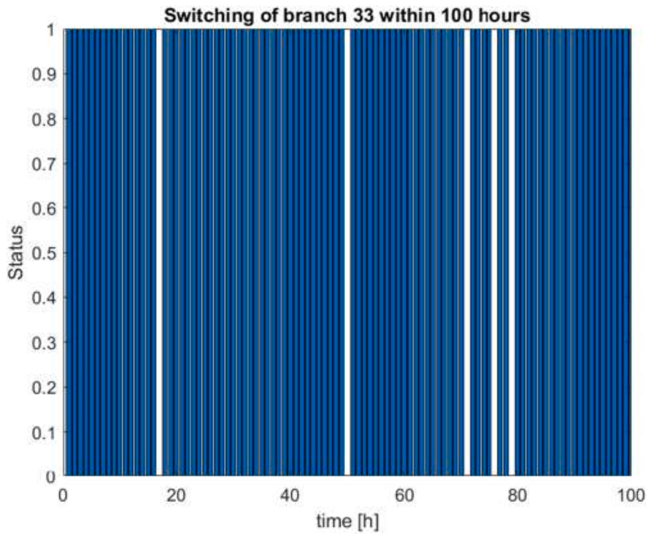

Fig. 24. Hourly closing/opening of branch 33, Scenario 1 for first 100 h.

the presence of distributed energy sources and storage systems. The reconfiguration is performed by Minimum Spanning Tree, Kruskal algorithm, followed by capacitor switching by Simulated Annealing. In undertaken analyses BESS and DG are present from the very start, in initial configuration of 118 node, 132 branch analyzed network (of 15 tie switches). Large number of real constraints are considered, particularly the number of commutations per switching element within 24 h. This is very important from a technical aspect. The network is represented realistically as hourly changes in production and consumption are considered. Kruskal algorithm was first tested and compared with other algorithms concerning reconfiguration for active power loss reduction. It proved to be extremely fast and sufficiently accurate in the calculation of the configuration, qualifying it for use in computation. A special focus of the paper is on the use of Battery Energy Storage Systems in distribution network. Discussion is given to underscore the point of BESS connection and the optimal power required.

Three Scenarios are discused. The first one is with BESS, the second one is without BESS, and the third one is original network only with DGs. Scenario with BESS (Scenario 1) is more costly than analog that has not them but also better in terms of expeneses. The cost of electrical energy loss is $17,316 (better than without BESS by $12), the cost of unsupplied electrical energy is $6476,000 (better than without BESS by $10,400), and the cost of peak power losses is $176,570 (better than without BESS by $390). This is because of excessive fee for BESS charging and discharging ($29,672). It can be concluded that improper placement of distributed sources and BESS can lead to excessive currents, overvoltages, undervoltages, and power flow reversal. The conclusion of the detailed analyses shows that the correct use of these systems results in technically optimal solution but that can be more expensive regarding final cost. The cheapest is Scenario 2, which does not have BESS, and it is cheaper than the identical scenario with BESS for $18,600. Conclusion can be drawn that addition of Battery Energy Storage Systems makes full technical sense, especially concerning the cost of unsupplied electrical energy albeit being more expensive.

The new algorithm gives the cheapest solution with minimum power

Table 4
Capacitor price step up function.

CB	> 0, ≤ 300 kVAr	> 300, ≤ 600 kVAr	> 600, ≤ 900 kVAr	> 900, ≤1200 kVAr	> 1200 kVAr
price	1900 $	3200 $	4500 $	5400 $	6000 $

Maintenance and installation cost is included in fixed part of the price.

Table 5
Comparison analysis supported with quantitative indicators.

Ref	Neworks	Number of cases	min Ploss or Eloss
[14]	16 and 33	3	56.24 kW and 126.31 kW
[15]	7, 10, 12, 16, 28 and 30-bus networks	3	0.874 MWh, 438.577 MWh, 1.435 MWh, 936.186 MWh, 41.618 MWh, 561.989 MWh
[17]	33	3	139.53 kW
[21]	34	3	1752 kWh
[22]	33 and 69	2	74.45 kW and 70.52 kW
[24]	33 and 123	2	202.7 kW and 478.20 kW
[25]	33 and 69	5	70.348 kW and 42.769 kW
[26]	33 and 69	5	77.01 kW and 13.35 kW
[27]	33, 70 and 118	3	66.4 kW, 99.9 kW, 375.2 kW
[34]	69 and 118	4	48.62 kW and 340.12 kW
[35]	16, 37 and 1069	3	26.622 kW, 51.868 kW, 79.168 kW
proposed	118	3	253 kW

Table 6
Presentation of part of the previous literature in the field of reconfiguration and compensation with the presence of distributed sources in accordance with the parameters discussed in the articles.

Ref	VP 1	EI 2	LU 3	CP 4	LM 5	DGW 6	DGS 7	CBC 8	BESS 9
[14]				x	x				
[15]		x		x	x	biomass		x	
[16]	x	x			x	x			x
[17]	x	x			x		x	x	x
[18]	x			x		x	x		
[19]					x	x			
[20]		x					x		x, HES
[21]	x			x	x		x		x
[22]	x	x			x	x			
[24]	x		x	x	x	x			
[25]	x				x	x			
[26]	x				x	x			
[27]					x	x	x		
[33]	x	x		x	x	x	x	x	
[34]				x	x	x			
[35]			x		x				
proposed	x	x		x	x	x	x	x	x

Table 3
Results for 1008 h of operation for different scenarios.

Scenario	U slack node	Energysavings	Commutations	ΔIstart	ΔIfinal	Umax start	Umax final	Umin final	Cost of unsupplied electric energy
No	p.u.	$	$	A	A	p.u.	p.u.	p.u.	$
1 (yes BESS yes DG yes CB yes OLTC)	1.05	1 168 185 **1 109 924**	1189 **59 450**	81.0613	88.3938	1.05	1.05	0.9688	6 476 000
2 (no BESS yes DG yes CB yes OLTC)	1.05	1 186 785 **1 115 294**	1459 **72 950**	74.8565	82.1007	1.05	1.0519	0.9688	6 486 400
3 (no BESS yes DG no CB no OLTC)	1.000	0	–	−17.6153	−17.6153	1	1	0.7813	7 430 700

Note: non-bold figures refer to the price of $1, and bold figures to $50 per commutation,.

losses for capacitor banks. The final results show that only 1200 kVAr, then 600 kVAr and at the end 300 kVAr batteries were assigned to the respective nodes. The 1200 kVAr banks are connected to nodes 50, 74, 82, 97 and 111. On the other hand, a 600 kVAr bank is connected only to node 53 and the 300 kVAr banks are connected to nodes 19, 47 and 70. Finally, wind generators and BESS are associated to the nodes 34 and 102, and PV panels are included in the nodes 50 and 111.

The originality of the paper is considered with proper analyses of BESS (with unique charging/discharging presentation) which reflect the future of distribution networks and On Load Tap Changer inclusion in the reconfiguration (with branch limited number of commutations) and capacitor placement problem. This algorithm could be useful for planers where the capacitor banks could be and how hourly reconfiguration should look like. This paper doesn't discuss reconfiguration changing during the time because of the faults and unpredicted events. Positions of the BESS are commented in separate chapter as a contribution and result of special research. These locations are fixed during reconfiguration simulations.

CRediT authorship contribution statement

Tomislav Rajić: Writing – original draft, Visualization, Supervision, Methodology, Formal analysis. **Branko Stojanović:** Writing – review & editing, Supervision, Methodology, Investigation.

Declaration of competing interest

The authors declare that they have no known competing financial interests or personal relationships that could have appeared to influence the work reported in this paper.

Acknowledgements

This work was financially supported by the Ministry of Science, Technological Development and Innovation of the Republic of Serbia under contract number: 451-03-65/2024-03/200103.

Appendix. Appendix

Table A1

Table A1
Input data and MATPOWER power flow calculation results for initial configuration, 100 MVA base power, 11 kV Un, nodal lowest voltage is shaded.

branch no.	branch	R (p. u.)	X (p. u.)	nodal active load (MW)	nodal reactive load (MVAr)	| V | p. u.	brunch active power loss Ploss (MW)	branch reactive power loss Qloss (MVAr)
1	1-2	0,0298	0,0107	0,13384	0,10114	0,996	0,055	0,02
2	2-3	0,0273	0,0098	0,016214	0,011292	0,996	0,000	0,00
3	2-4	0,0372	0,0134	0,034315	0,021845	0,992	0,043	0,02
4	4-5	0,0124	0,0446	0,073016	0,063602	0,992	0,000	0,00
5	5-6	0,0124	0,0446	0,14420	0,068604	0,992	0,000	0,00
6	6-7	0,0124	0,0103	0,10447	0,061725	0,992	0,000	0,00
7	7-8	0,0149	0,0116	0,028547	0,011503	0,992	0,000	0,00
8	8-9	0,0174	0,0521	0,087560	0,051073	0,991	0,000	0,00
9	2-10	0,1372	0,1111	0,19820	0,10677	0,991	0,009	0,01
10	10-11	0,0926	0,0652	0,14680	0,075995	0,989	0,005	0,00
11	11-12	0,1545	0,2587	0,026040	0,018687	0,988	0,000	0,00
12	12-13	0,1174	0,1250	0,052100	0,023220	0,987	0,000	0,00
13	13-14	0,1488	0,0975	0,14190	0,11750	0,986	0,000	0,00
14	14-15	0,1240	0,0372	0,021870	0,028790	0,986	0,000	0,00
15	15-16	0,1322	0,1488	0,03370	0,026450	0,986	0,000	0,00
16	16-17	0,1298	0,1413	0,032430	0,025230	0,986	0,000	0,00
17	11-18	0,1802	0,2355	0,020234	0,011906	0,984	0,006	0,01
18	18-19	0,0975	0,1529	0,15694	0,078523	0,981	0,003	0,00
19	19-20	0,1322	0,1620	0,54629	0,35140	0,978	0,003	0,00
20	20-21	0,0992	0,1562	0,18031	0,16420	0,976	0,001	0,00
21	21-22	0,0992	0,0652	0,093167	0,054594	0,975	0,000	0,00
22	22-23	1,1653	0,5975	0,085180	0,039650	0,968	0,004	0,00
23	23-24	0,2421	0,1114	0,16810	0,095178	0,967	0,001	0,00
24	24-25	0,1099	0,0860	0,12511	0,15022	0,967	0,000	0,00
25	25-26	0,1471	0,1107	0,016030	0,024620	0,966	0,000	0,00
26	26-27	0,1471	0,1107	0,026030	0,024620	0,966	0,000	0,00
27	4-28	0,0124	0,0245	0,59456	0,52262	0,989	0,013	0,03
28	28-29	0,0099	0,0228	0,12062	0,059117	0,987	0,009	0,02
29	29-30	0,0992	0,2286	0,10238	0,099554	0,973	0,038	0,09
30	30-31	0,1736	0,2008	0,51340	0,31850	0,961	0,041	0,05
31	31-32	0,0992	0,0446	0,47525	0,45614	0,956	0,018	0,01
32	32-33	0,1471	0,1934	0,15143	0,13679	0,948	0,019	0,02
33	33-34	0,1471	0,1934	0,20538	0,083302	0,940	0,016	0,02
34	34-35	0,1273	0,1339	0,13160	0,093082	0,934	0,012	0,01
35	30-36	0,1545	0,2157	0,44840	0,36979	0,970	0,002	0,00
36	36-37	0,1099	0,0818	0,44052	0,32164	0,970	0,000	0,00
37	29-38	0,2727	0,1603	0,11254	0,055134	0,981	0,011	0,01
38	38-39	0,2562	0,1603	0,053963	0,038998	0,975	0,009	0,01
39	39-40	0,1074	0,1603	0,39305	0,34260	0,972	0,004	0,01
40	40-41	0,2314	0,1240	0,32674	0,27856	0,968	0,004	0,00
41	41-42	09752	0,7025	0,53626	0,24024	0,958	0,008	0,01
42	42-43	0,3471	0,2031	0,076247	0,06652	0,957	0,000	0,00

(continued on next page)

Table A1 (*continued*)

43	43-44	0,2231	0,0803	0,053520	0,039760	0,956	0,000	0,00
44	44-45	0,2802	0,1009	0,040328	0,031964	0,956	0,000	0,00
45	45-46	0,2231	0,1470	0,039653	0,020758	0,956	0,000	0,00
46	35-47	0,1736	0,1143	0,066195	0,042361	0,928	0,015	0,01
47	47-48	0,0992	0,0652	0,073904	0,051653	0,925	0,008	0,01
48	48-49	0,1240	0,0816	0,11477	0,057965	0,921	0,009	0,01
49	49-50	0,1240	0,0816	0,91837	1,2015	0,917	0,009	0,01
50	50-51	0,1983	0,1307	0,21030	0,14666	0,914	0,002	0,00
51	51-52	0,0992	0,0652	0,066680	0,056608	0,914	0,001	0,00
52	52-53	0,3347	0,1205	0,042207	0,040184	0,911	0,001	0,00
53	53-54	0,3347	0,1205	0,43374	0,28341	0,909	0,001	0,00
54	29-55	0,3231	0,1165	0,062100	0,026860	0,984	0,004	0,00
55	55-56	0,3355	0,1207	0,092460	0,088380	0,980	0,004	0,00
56	56-57	0,3355	0,1207	0,085188	0,055436	0,977	0,003	0,00
57	57-58	0,5835	0,4513	0,34530	0,33240	0,971	0,004	0,00
58	58-59	0,2793	0,1007	0,022500	0,016830	0,970	0,000	0,00
59	59-60	0,2793	0,1007	0,080551	0,049156	0,969	0,000	0,00
60	60-61	0,1711	0,0617	0,095860	0,090758	0,968	0,000	0,00
61	61-62	0,2041	0,7374	0,062920	0,047700	0,968	0,000	0,00
62	1-63	0,0231	0,0345	0,47880	0,46374	0,996	0,021	0,03
63	63-64	0,0967	0,1666	0,12094	0,052006	0,981	0,078	0,13
64	64-65	0,2107	0,0759	0,13911	0,10034	0,968	0,076	0,03
65	65-66	0,1736	0,0627	0,39178	0,19350	0,961	0,026	0,01
66	66-67	0,3165	0,1140	0,027741	0,026713	0,949	0,038	0,01
67	67-68	0,4165	0,2730	0,052814	0,025257	0,932	0,048	0,03
68	68-69	0,3355	0,1207	0,066890	0,038713	0,921	0,038	0,01
69	69-70	0,7950	0,6289	0,46750	0,39514	0,888	0,085	0,07
70	70-71	0,1364	0,0496	0,59485	0,23974	0,884	0,009	0,00
71	71-72	0,2504	0,0902	0,13250	0,084363	0,879	0,009	0,00
72	72-73	0,2504	0,0902	0,052699	0,022482	0,875	0,007	0,00
73	73-74	0,1702	0,1190	0,86979	0,614775	0,871	0,004	0,00
74	74-75	0,1926	0,0694	0,031349	0,029817	0,871	0,000	0,00
75	75-76	0,4884	0,1465	0,19239	0,12243	0,869	0,001	0,00
76	76-77	0,1041	0,0374	0,065750	0,045370	0,869	0,000	0,00
77	64-78	0,4620	0,3047	0,23815	0,22322	0,965	0,037	0,02
78	78-79	0,1537	0,1014	0,29455	0,16247	0,960	0,010	0,01
79	79-80	0,1537	0,1014	0,48557	0,43792	0,957	0,004	0,00
80	80-81	0,2149	0,1149	0,24353	0,18303	0,955	0,002	0,00
81	81-82	0,1273	0,1223	0,24353	0,18303	0,954	0,000	0,00
82	82-83	0,1901	0,1058	0,13425	0,11929	0,954	0,000	0,00
83	83-84	0,2083	0,0876	0,022710	0,027960	0,953	0,000	0,00
84	84-85	0,1488	0,1223	0,49513	0,026515	0,953	0,000	0,00
85	79-86	0,1322	0,1504	0,38378	0,25716	0,959	0,000	0,00
86	86-87	0,1653	0,1901	0,049640	0,020600	0,959	0,000	0,00
87	87-88	0,1322	0,3248	0,022473	0,011806	0,959	0,000	0,00
88	65-89	0,5529	0,1993	0,062930	0,042960	0,957	0,021	0,01
89	89-90	0,2198	0,1014	0,030670	0,034930	0,952	0,008	0,00
90	90-91	0,2198	0,1014	0,062530	0,066790	0,948	0,007	0,00
91	91-92	0,2198	0,1014	0,11457	0,081748	0,947	0,000	0,00
92	92-93	0,2198	0,1014	0,081292	0,066526	0,946	0,000	0,00
93	93-94	0,1926	0,0950	0,031733	0,015960	0,946	0,000	0,00
94	94-95	0,4099	0,1140	0,033320	0,060480	0,946	0,000	0,00
95	91-96	0,1620	0,1488	0,53128	0,22485	0,945	0,003	0,00
96	96-97	0,1620	0,1488	0,50703	0,36742	0,943	0,001	0,00
97	97-98	0,1542	0,1008	0,26390	0,011700	0,943	0,000	0,00
98	98-99	0,0617	0,2628	0,045990	0,030392	0,943	0,000	0,00
99	1-100	0,0517	0,0219	0,10066	0,047572	0,996	0,024	0,01
100	100-101	0,1240	0,1934	0,45648	0,35030	0,983	0,046	0,07
101	101-102	0,1113	0,0734	0,52256	0,44929	0,976	0,033	0,02
102	102-103	0,1907	0,0994	0,40843	0,16846	0,966	0,043	0,02
103	103-104	0,3694	0,1329	0,14148	0,13425	0,950	0,069	0,02
104	104-105	0,1349	0,0486	0,10443	0,066024	0,944	0,023	0,01
105	105-106	0,2727	0,0818	0,096793	0,083647	0,934	0,044	0,01
106	106-107	0,1289	0,0464	0,49392	0,41934	0,929	0,019	0,01
107	107-108	0,3156	0,1136	0,22538	0,13588	0,919	0,032	0,01
108	108-109	0,1344	0,0483	0,50921	0,38721	0,915	0,011	0,00
109	109-110	0,3156	0,1136	0,18850	0,17346	0,908	0,015	0,01

(*continued on next page*)

Table A1 (*continued*)

110	110-111	0,2021	0,0726	0,91803	0,89855	0,905	0,004	0,00
111	110-112	0,1726	0,0622	0,30508	0,21537	0,907	0,000	0,00
112	112-113	0,1902	0,0684	0,054380	0,040970	0,907	0,000	0,00
113	100-114	0,5043	0,1815	0,21114	0,19290	0,993	0,002	0,00
114	114-115	0,1542	0,1050	0,067009	0,053336	0,992	0,000	0,00
115	115-116	0,3084	0,2033	0,16207	0,090321	0,991	0,000	0,00
116	116-117	0,3347	0,3033	0,048785	0,029156	0,991	0,000	0,00
117	117-118	0,4041	0,3620	0,033900	0,018980	0,991	0,000	0,00
118	27-46	0,4345	0,2417					
119	17-27	0,4345	0,2410					
120	8-24	0,3531	0,1272					
121	43-54	0,3967	0,1428					
122	49-62	0,2975	0,1071					
123	37-62	0,4711	0,4727					
124	9-40	0,4380	0,2767					
125	58-96	0,3270	0,1178					
126	73-91	0,5620	0,5355					
127	75-88	0,3357	0,1210					
128	77-99	0,3823	0,1383					
129	83-108	0,5380	0,1934					
130	86-105	0,6715	0,2417					
131	110-118	0,5859	0,2110					
132	25-35	0,4132	0,4132					

Adopted maximum branch thermal current limits are: 1 (1.9 kA), 2 (0.9 kA), 3 (1.85 kA), 4–7 (0.95 kA), 8–26 (0.9 kA), 27 and 28 (1.45 kA), 29–34 (1.25 kA), 35–45 (0.9 kA), 46–53 (1.25 kA), 54–61 (0.9 kA), 62 and 63 (1.45 kA), 64–76 (1.25 kA), 77–98 (0.9 kA), 99–109 (1.25 kA), 110 (0.9 kA), 111 and 112 (1.25 kA) and 113–132 (0.9 kA), numbers outside the brackets denote branch ordinal number.

Data availability

The authors do not have permission to share data.

References

[1] F. Dalavi, M.E.H. Golshan, N.D. Hatziargyriou, A review on topology identification methods and applications in distribution networks, Electr. Power Syst. Res. 234 (2024) 110538, https://doi.org/10.1016/j.epsr.2024.110538.

[2] M.R. Behbahani, A. Jalilian, A. Bahmanyar, D. Ernst, Comprehensive review on static and dynamic distribution network reconfiguration methodologies, IEEE Access., 12 (2024) 9510–9525. 10.1109/ACCESS.2024.3350207.

[3] S. Civanlar, J.J. Grainger, H. Yin, S.S.H. Lee, Distribution feeder reconfiguration for loss reduction, IEEE Trans. Power Deliv. 3 (1988) 1217–1223, https://doi.org/10.1109/61.193906.

[4] A. Bayat, Uniform voltage distribution based constructive algorithm for optimal reconfiguration of electric distribution networks, Electr. Power Syst. Res. 104 (2013) 146–155, https://doi.org/10.1016/j.epsr.2013.06.010.

[5] A.R. Abul Wafa, A new heuristic approach for optimal reconfiguration in distribution systems, Electr. Power Syst. Res. 81 (2011) 282–289, https://doi.org/10.1016/j.epsr.2010.09.003.

[6] D. Shirmohammadi, H.W. Hong, Reconfiguration of electric distribution networks for resistive line losses reduction, IEEE Trans. Power Deliv. 4 (1989) 1492–1498, https://doi.org/10.1109/61.25637.

[7] H.D. Chiang, R.J. Jumeau, Optimal network reconfigurations in distribution systems: Part 2: solution algorithms and numerical results, IEEE Trans. Power Deliv. 5 (1990) 1568–1574, https://doi.org/10.1109/61.58002.

[8] H.D. Chiang, R.J. Jumeau, Optimal network reconfigurations in distribution systems: part 1: A new formulation and a solution methodology, IEEE Trans. Power Deliv. 5 (1990) 1902–1909, https://doi.org/10.1109/61.103687.

[9] A. Asrari, S. Lotfifard, M.S. Payam, Pareto dominance-based multiobjective optimization method for distribution network reconfiguration, IEEE Trans. Smart. Grid. 7 (2016) 1401–1410, https://doi.org/10.1109/TSG.2015.2468683.

[10] Z. Li, S. Jazebi, F. de Leon, Determination of the optimal switching frequency for distribution system reconfiguration, IEEE Trans. Power Deliv. 32 (2017) 2060–2069, https://doi.org/10.1109/TPWRD.2016.2594385.

[11] A. Augugliaro, L. Dusonchet, M.G. Ippolito, E.R. Sanseverino, Minimum losses reconfiguration of MV distribution networks through local control of tie-switches, IEEE Trans. Power Deliv. 18 (2003) 762–771, https://doi.org/10.1109/TPWRD.2003.813801.

[12] S.S.F. Souza, R. Romero, J.F. Franco, Artificial immune networks Copt-aiNet and Opt-aiNet applied to the reconfiguration problem of radial electrical distribution systems, Electr. Power Syst. Res. 119 (2015) 304–312, https://doi.org/10.1016/j.epsr.2014.10.012.

[13] E.R. Ramos, J.R. Santos, J. Reyes, A simpler and exact mathematical model for the computation of the minimal power losses tree, Electr. Power Syst. Res. 80 (2010) 562–571, https://doi.org/10.1016/j.epsr.2009.10.016.

[14] M. Mahdavi, A. Awaafo, M. Dini, S. Moradi, F. Jurado, D. Vera, A flexible loss reduction formulation for simultaneous capacitor placement and network reconfiguration in distribution grids, Electr. Power Syst. Res. 235 (2024) 8, https://doi.org/10.1016/j.epsr.2024.110708, pgs.

[15] M. Mahdavi, A. Awaafo, S.Z. Djokić, F. Jurado, An innovative power loss and cost minimization framework for distribution networks with uncertain variable loads by coordinating reconfiguration, capacitor installation and renewable generators placement, IEEE Trans. Ind. Appl. 60 (2024) 7500–7510, https://doi.org/10.1109/TIA.2024.3403958.

[16] Z. Li, S. Wang, Y. Zhou, W. Liu, X. Zheng, Optimal distribution systems operation in the presence of wind power by coordinating network reconfiguration and demand response, Int. J. Electr. Power Energy Syst. 119 (2020) 105911, https://doi.org/10.1016/j.ijepes.2020.105911.

[17] S.M. Razavi, H.R. Momeni, M.R. Haghifam, S. Bolouki, Multi-objective optimization of distribution networks via daily reconfiguration, IEEE Trans. Power Deliv. 37 (2021) 775–785, https://doi.org/10.1109/TPWRD.2021.3070796.

[18] P. Agrawal, N. Kanwar, N. Gupta, K.R. Niazi, A. Swarnkar, Resiliency in active distribution systems via network reconfiguration, Sustain. Energy Grids Netw. 26 (2021) 100434, https://doi.org/10.1016/j.segan.2021.100434.

[19] L. Ibarra, J. Aviles, D. Guillen, J.C. Mayo-Maldonado, J.E. Valdez-Resendiz, P. Ponce, Optimal micro-PMU placement and virtualization for distribution network changing topologies, Sustain. Energy Grids Netw. 27 (2021) 100510, https://doi.org/10.1016/j.segan.2021.100510.

[20] M. Miller, J.L. Paternina, S.F. Contreras, C.A. Cortes, J.M.A. Myrzik, Optimal allocation of renewable energy systems in a weak distribution network, Electr. Power Syst. Res. 235 (2024) 110649, https://doi.org/10.1016/j.epsr.2024.110649.

[21] J.J.A. Saldanha, A. Nied, R. Trentini, R. Kutzner, AI-based optimal allocation of BESS, EV charging station and DG in distribution network for losses reduction and peak load shaving, Electr. Power Syst. Res. 234 (2024) 110554, https://doi.org/10.1016/j.epsr.2024.110554.

[22] H. Prasad C, K. Subbaramaiah, P. Sujatha, Optimal DG unit placement in distribution networks by multi-objective whale optimization algorithm & its techno-economic analysis, Electr. Power Syst. Res. 214 (Part A) (2023) 108869, https://doi.org/10.1016/j.epsr.2022.108869.

[23] N. Kovački, P. Vidović, A. Sarić, Scalable algorithm for the dynamic reconfiguration of the distribution network using the Lagrange relaxation approach, Int. J. Electr. Power Energy Syst. 94 (2018) 188–202, https://doi.org/10.1016/j.ijepes.2017.07.005.
[24] S.K. Paul, A. Mohapatra, D. Chandra Das, A new continuous variables and convex relaxation based formulation for reconfiguration of unbalanced mutually coupled active distribution networks, Electr. Power Syst. Res. 228 (2024) 110009, https://doi.org/10.1016/j.epsr.2023.110009.
[25] P. Moghari, R.M. Chabanloo, H. Torkaman, Distribution system reconfiguration based on MILP considering voltage stability, Electr. Power Syst. Res. 222 (2023) 109523, https://doi.org/10.1016/j.epsr.2023.109523.
[26] M. Mahdavi, A. Awaafo, M. Dini, S. Moradi, F. Jurado, D. Vera, Simultaneous feeder reconfiguration and distributed generation planning in the presence of voltage-dependent and variable loads, Electr. Power Syst. Res. 235 (2024) 110783, https://doi.org/10.1016/j.epsr.2024.110783.
[27] M. Mahdavi, K. Erich, K. Schmitt, F. Jurado, Robust distribution network reconfiguration in the presence of distributed generation under uncertainty in demand and load variations, IEEE Trans. Power Deliv. 38 (2023) 3480–3495, https://doi.org/10.1109/TPWRD.2023.3277816.
[28] H.D. Chiang, J.C. Wang, O. Cockings, H.D. Shin, Optimal capacitor placements in distribution systems: Part 1: A new formulation and the overall problem, IEEE Trans. Power Deliv. 5 (1990) 634–642, https://doi.org/10.1109/61.53065.
[29] H. Ahmadi, J.R. Marti, Minimum-loss network reconfiguration: A minimum spanning tree problem, Sustain. Energy Grids Netw. 1 (2014) 1–9, https://doi.org/10.1016/j.segan.2014.10.001.
[30] B. Stojanović, R. Tomislav, Distribution network reconfiguration and capacitor switching in the presence of wind generators, Electr. Eng. 104 (2022) 2249–2266, https://doi.org/10.1007/s00202-021-01470-8.
[31] N. Mithulananthan, D.Q. Hung, K.Y. Lee, Intelligent Network Integration of Distributed Renewable Generation, 1st Edition, Springer, 2017.
[32] D. Zhang, Z. Fu, L. Zhang, An improved TS algorithm for loss-minimum reconfiguration in large-scale distribution systems, in: Electr. Power Syst. Res., 77, 2007, pp. 685–694, https://doi.org/10.1016/j.epsr.2006.06.005.
[33] B. Stojanović, T. Rajić, D. Šošić, Distribution network reconfiguration and reactive power compensation using a hybrid simulated annealing – Minimum spanning tree algorithm, Int. J. Electr. Power Energy Syst. 147 (2023) 108829, https://doi.org/10.1016/j.ijepes.2022.108829.
[34] K. Muthukumar, S. Jayalalitha, Integrated approach of network reconfiguration with distributed generation and shunt capacitors placement for power loss minimization in radial distribution networks, Appl. Soft Comput. 52 (2017) 1262–1284, https://doi.org/10.1016/j.asoc.2016.07.031.
[35] Y. Qu, C.C. Liu, J. Xu, Y. Sun, S. Liao, D. Ke, A global optimum flow pattern for feeder reconfiguration to minimize power losses of unbalanced distribution systems, Int. J. Electr. Power Energy Syst. 131 (2021) 107071, https://doi.org/10.1016/j.ijepes.2021.107071.
[36] D.K. Khatod, V. Pant, J. Sharma, Evolutionary programming based optimal placement of renewable distributed generators, IEEE Trans. Power. Syst. 28 (2) (2013) 683–695, https://doi.org/10.1109/tpwrs.2012.2211044.